AD-A070 791 ILLINOIS UNIV AT URBANA-CHAMPAIGN ELECTROMAGNETICS LAB F/G 9/5
AN IMPROVED THEORY FOR MICROSTRIP ANTENNAS AND APPLICATIONS. PA--ETC(U)
MAY 79 Y T LO, W F RICHARDS, D D HARRISON F19628-78-C-0025

UNCLASSIFIED UIEM-78-18-PT-1 RADC -TR-79-111-PT-1 NL

| OF |
AD
A070791

END
DATE
FILMED
8 -79
DDC

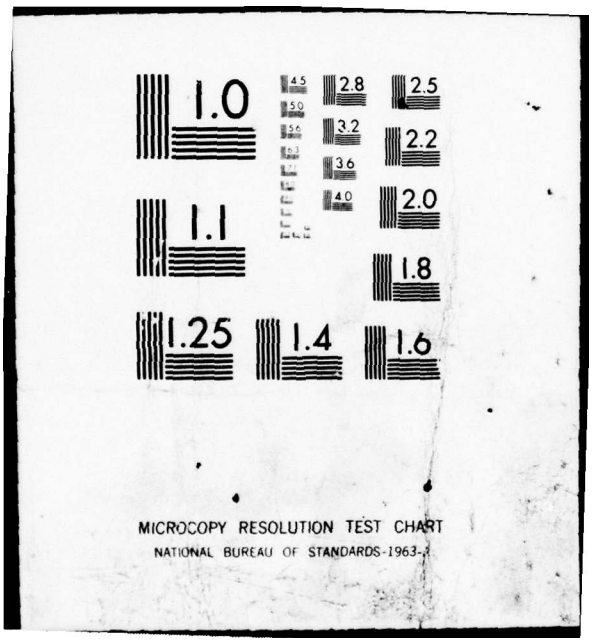
1.0
1.1
1.25
1.4
1.6
1.8
2.0
2.2
2.5
2.8
3.2
3.6
4.0
4.5
5.0
5.6
MICROCOPY RESOLUTION TEST CHART
NATIONAL BUREAU OF STANDARDS-1963-A

RADC-TR-79-111
Interim Report
May 1979

LEVEL

AN IMPROVED THEORY FOR MICROSTRIP ANTENNAS AND APPLICATIONS - PART I

University of Illinois

Y. T. Lo
W. F. Richards
D. D. Harrison

ROME AIR DEVELOPMENT CENTER
Air Force Systems Command
Griffiss Air Force Base, New York 13441

This report has been reviewed by the RADC Information Office (OI) and is releasable to the National Technical Information Service (NTIS). At NTIS it will be releasable to the general public, including foreign nations.

RADC-TR-79-111 has been reviewed and is approved for publication.

APPROVED: John A. Strom

JOHN A. STROM
Contract Monitor

APPROVED: Allan C. Schell

ALLAN C. SCHELL
Chief, Electromagnetic Sciences Division

FOR THE COMMANDER: John P. Huss

JOHN P. HUSS
Acting Chief, Plans Office

If your address has changed or if you wish to be removed from the RADC mailing list, or if the addressee is no longer employed by your organization, please notify RADC (EEA) Hanscom AFB MA 01731. This will assist us in maintaining a current mailing list.

Do not return this copy. Retain or destroy.

UNCLASSIFIED

SECURITY CLASSIFICATION OF THIS PAGE *(When Data Entered)*

REPORT DOCUMENTATION PAGE

READ INSTRUCTIONS BEFORE COMPLETING FORM

1. REPORT NUMBER: RADC-TR-79-111-PT-1	2. GOVT ACCESSION NO.
3. RECIPIENT'S CATALOG NUMBER	
4. TITLE *(and Subtitle)*: AN IMPROVED THEORY FOR MICROSTRIP ANTENNAS AND APPLICATIONS. PART I.	5. TYPE OF REPORT & PERIOD COVERED: Interim Report, no 1.,
	6. PERFORMING ORG. REPORT NUMBER: EM-78-18, UILU-ENG-78-2563
7. AUTHOR(s): Y. T. Lo, W. F. Richards, D. D. Harrison	8. CONTRACT OR GRANT NUMBER(s): F19628-78-C-0025 new
9. PERFORMING ORGANIZATION NAME AND ADDRESS: University of Illinois at Urbana-Champaign, Dept of Electrical Engineering/Electromagnetics Lab, Urbana IL 61801	10. PROGRAM ELEMENT, PROJECT, TASK AREA & WORK UNIT NUMBERS: 61102F; 2305J323; J3
11. CONTROLLING OFFICE NAME AND ADDRESS: Deputy for Electronic Technology (RADC/EEA), Hanscom AFB MA 01731	12. REPORT DATE: May 1979
	13. NUMBER OF PAGES: 31
14. MONITORING AGENCY NAME & ADDRESS *(if different from Controlling Office)*: Same; UIEM-78-18-PT-1, UILU-ENG-78-2563-PT-1	15. SECURITY CLASS. *(of this report)*: UNCLASSIFIED
	15a. DECLASSIFICATION/DOWNGRADING SCHEDULE

16. DISTRIBUTION STATEMENT *(of this Report)*

Approved for public release; distribution unlimited.

32p.

17. DISTRIBUTION STATEMENT *(of the abstract entered in Block 20, if different from Report)*

Same

18. SUPPLEMENTARY NOTES

RADC Project Engineers: John A. Strom and Nicholas Kernweis (EEA)

19. KEY WORDS *(Continue on reverse side if necessary and identify by block number)*

Microstrip Antennas, Excitation of cavity and input impedance, Multiport Microstrip Antennas, Circularly Polarized Microstrip Antennas, Circuit representation of microstrip antennas

20. ABSTRACT *(Continue on reverse side if necessary and identify by block number)*

An improvement to a recently reported theory for the analysis of the pattern and impedance loci of microstrip antennas is developed. It yields a theory which is simple and inexpensive to apply. The fields in the interior of the antennas are characterized in terms of a discrete set of modes. The poles corresponding to these modes are complex and depend on the losses in the antenna. The representation of the fields in terms of these modes is rigorous only for a bona fide cavity with no copper loss. The proper shift in the complex poles due to the

DD FORM 1 JAN 73 1473

UNCLASSIFIED 408102

SECURITY CLASSIFICATION OF THIS PAGE *(When Data Entered)*

addition of copper and radiative losses is approximated by lumping the latter two together with the dielectric loss to form an effective loss tangent. By so doing, it is found that the resulting expressions for impedance of the microstrip antenna is in good agreement with measured results for all modes and feed locations. The theory is applied to the evaluation of impedance variation with feed location, multiport analysis, and to design of circularly polarized microstrip antennas.

TABLE OF CONTENTS

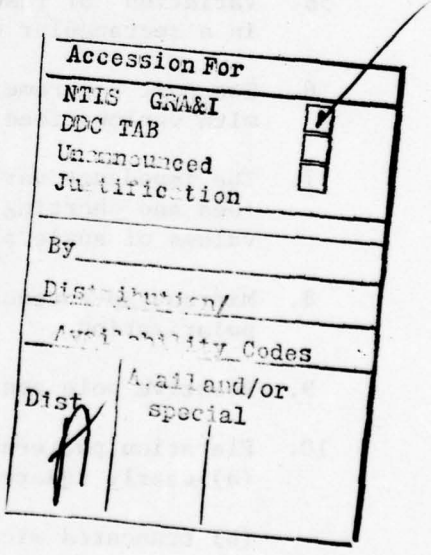

LIST OF FIGURES

AN IMPROVED THEORY FOR MICROSTRIP ANTENNAS AND APPLICATIONS

An improvement to a recently reported theory for the analysis of the pattern and impedance loci of microstrip antennas is developed. It yields a theory which is simple and inexpensive to apply. The fields in the interior of the antennas are characterized in terms of a discrete set of modes. The poles corresponding to these modes are complex and depend on the losses in the antenna. The representation of the fields in terms of these modes is rigorous only for a *bona fide* cavity with no copper loss. The proper shift in the complex poles due to the addition of copper and radiative losses is approximated by lumping the latter two together with the dielectric loss to form an effective loss tangent. By so doing, it is found that the resulting expressions for impedance of the microstrip antenna are in good agreement with measured results for all modes and feed locations. The theory is applied to the evaluation of impedance variation with feed location, multiport analysis, and to design of circularly polarized microstrip antennas.

I. *INTRODUCTION*

A number of recent papers have appeared on the subject of impedance and pattern prediction for microstrip antennas [1-5]. These papers represent basically four different approaches to the problem with differing degrees of flexibility, accuracy, and computational effort. The simplest approach, applicable to only rectangular microstrip antennas [1,2,3] involves treating the radiative properties of the latter as two parallel radiating slots interconnected by a low impedance transmission line. This approach will give fair agreement with the experimentiment in [2] as long as the feed point is chosen near one of the two "radiating edges," such as point 3 in Fig. 1a (in the 0,1 mode). However, if the feed is moved to some point between the edges, such as point 1 or 2 of the same figure, the theory predicts a locus symmetric about the real axis of the Smith chart. This is in contrast to the experimental results which show a strong shift of the locus into the inductive side of the Smith chart (see Fig. 1b). Thus, the method is not adequate for predicting impedance variation with feed location.

This theory, based on a simple slot-transmission line model that cannot be applied to geometries other than rectangles. This apparently has forced one author finally to follow the well known cavity approach in his study of disk antennas [2]. In these studies, it is generally assumed that the field inside the antenna is approximated by the dominant mode of the cavity derived from the antenna by inclosing its periphery by a magnetic wall. From this field, radiative and ohmic losses associat-

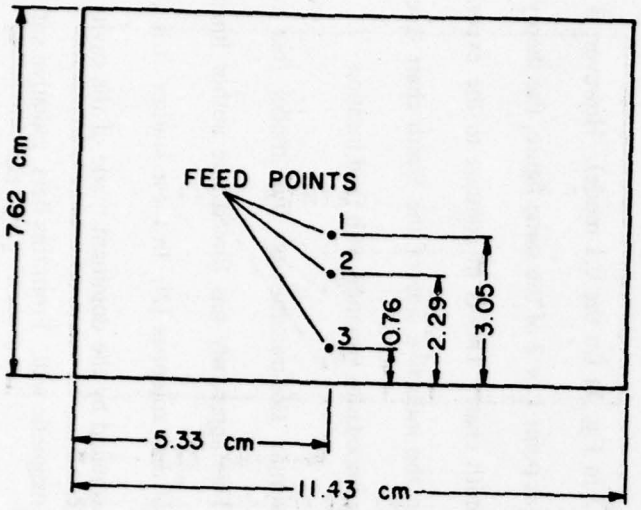

RECTANGULAR MICROSTRIP ANTENNA

SUBSTRATE: REXOLITE 2200
1/16" NOMINAL THICKNESS

(a)

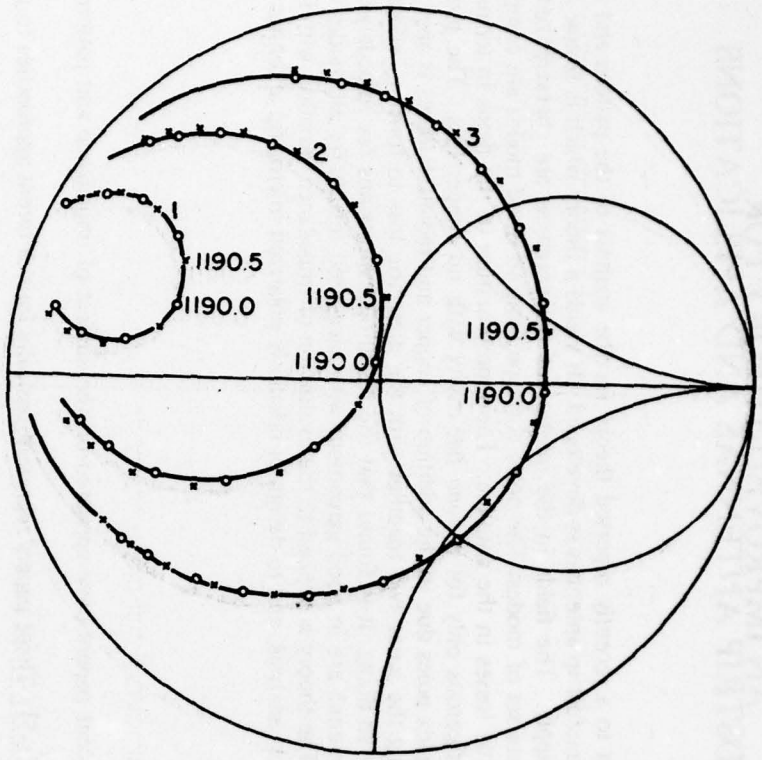

MEASURED LOCUS

× × COMPUTED LOCUS

INCREMENT: 5 MHz

(INCREASING FREQUENCY IS CLOCKWISE)

(b)

Fig. 1 (a) Dimensions and feed locations of rectangular microstrip antenna.
(b) Measured and computed impedance loci.

ed with the antenna are approximated together with stored energies. The conductance, G, and quality factor, Q, are computed at resonance and the impedance is found from $1/Z = [1 + jQ(f_0/f - f/f_0)]$ where f_0 is the resonant frequency. This approach also yields loci which are symmetric about the real axis of the Smith chart and hence do not accurately represent the impedance of the antenna at all feed points.

A third method [4] models the microstrip as a grid of wires and solves the resulting structure numerically. While this method seems to be somewhat more accurate and general, it is more costly to apply than necessary for most practical microstrips and provides little physical insight into the operation of these antennas.

A fourth method [5] replaces the antenna initially with a cavity as in the second approach discussed. However, in this case, a full modal expansion of the fields is applied. It is the neglecting of the non-resonant modes that causes much of the error in the first two methods. Inclusion of the effects of these modes yields computed loci which are shifted into the inductive side of the Smith chart, in agreement with the experiment. However, the approach used in [5] suffers some difficulties of its own when the dominant mode is not excited strongly enough. This paper is intended to provide a simple improvement to this theory which not only yields accurate results at any feed location, but also improves the computational efficiency. In addition, some applications of this theory to impedance matching, multiport analysis, and production of circularly polarized patterns are presented. It will be seen that in these applications, because of the strong frequency sensitivity, generally an accurate theory is needed. The excellent agreement with the experiment seems to suggest the validity of the theory.

II. *THEORY*

By assuming that the perimeter of the microstrip antenna can be inclosed in a perfect magnetic wall without much disturbing the field structure, one can expand the fields in modal functions ϕ_{mn} [5]. As an example, consider the rectangular microstrip shown in Fig. 2. The z directed electric field can

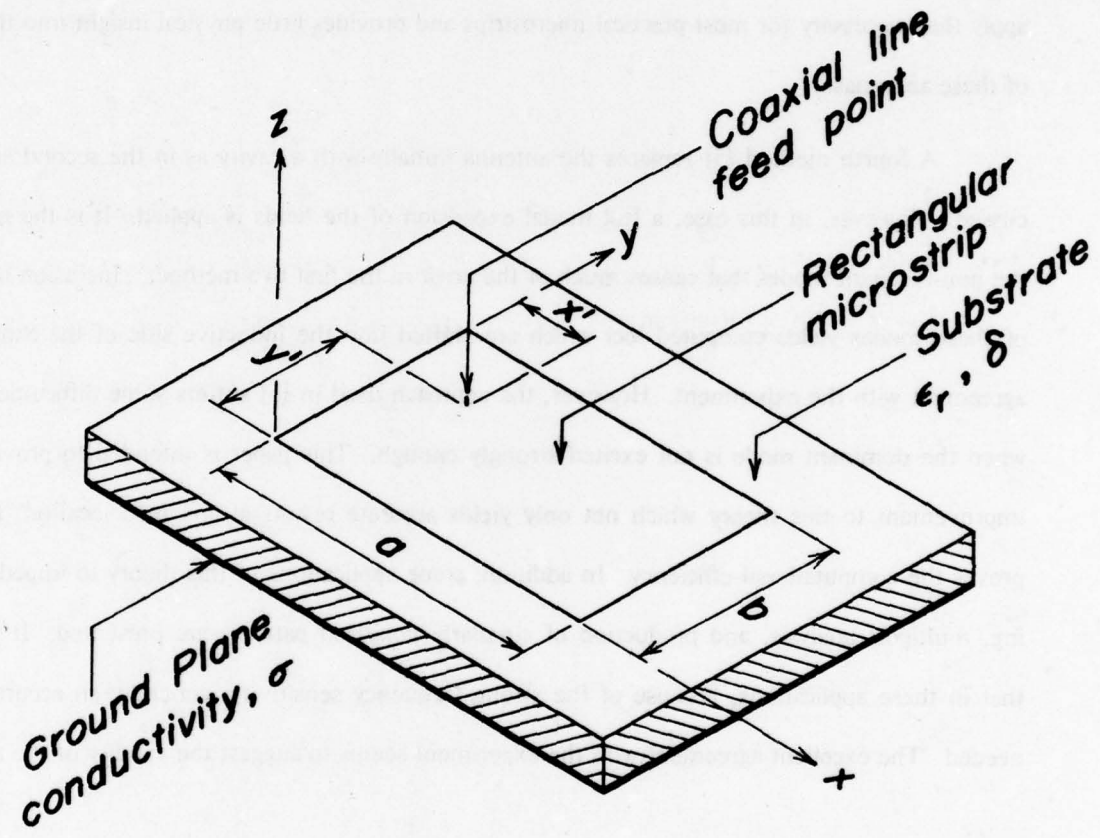

Fig. 2. Rectangular microstrip antenna.

thus be written as

$$E = jk_0\eta_0 \sum_{m=0}^{\infty}\sum_{n=0}^{\infty} \frac{\phi_{mn}(x,y)\phi_{mn}(x',y')}{k^2-k_{mn}^2}\, j_0\left(\frac{m\pi d}{2a}\right) \tag{1}$$

where $k^2 = \epsilon_r(1-j\delta)k_0^2$, $k_0 = 2\pi f/\nu$, f = frequency, ν = speed of light, ϵ_r = relative dielectric constant, δ = loss tangent of dielectric, $\eta_0 = 377\Omega$, $k_{mn}^2 = (m\pi/a)^2 + (n\pi/b)^2$, $j_0(x) = \sin(x)/x$, $\phi_{mn}(x,y) = \left(\frac{\epsilon_{0m}\epsilon_{0n}}{ab}\right)^{1/2} \cos(m\pi x/a)\cos(n\pi y/b)$, $\epsilon_{0m} = 1$ for $m=0$ and 2 for $m\neq 0$, and d is the "effective width" of a uniform strip of z directed source current of one amp. (The concept of effective feed width and its implications are discussed later). The inner series in (1) can be summed in closed form. This is equivalent to the mode-matching approach [5]. Once the field distribution has been obtained, a magnetic current source, $\mathbf{K}(x,y) = \hat{\mathbf{n}}\times\hat{\mathbf{z}}E(x,y)$ at the perimeter, with unit normal $\hat{\mathbf{n}}$, is defined. This source is allowed to radiate into space. The far field is computed for simplicity under the following additional approximations which have proven to give accurate results: a) Radiation due to electric surface currents induced on the patch and ground plane is negligible. b) The influence of the dielectric substrate on the radiation pattern can be ignored. c) The magnetic current ribbon is replaced by a magnetic line current on the ground plane of $t\mathbf{K}$. The surface wave trapped by the dielectric substrate is also computed from $\mathbf{K}$. From these, the radiated power P_{rad}, and the surface wave power P_{sw}, are found. Also, within the interior of the antenna, the power lost in the copper walls P_{Cu}, can be approximated as usual by assuming the currents that actually flow are the same as those under the condition of lossless walls. Finally, the power lost in the dielectric, P_d, within the antenna is easily computed.

From these losses, the input impedance, Z, can be computed by

$$1/Z = [P+j2\omega(W_E - W_M)]/|V|^2 \tag{2}$$

where $P = P_d + P_{Cu} + P_{sw} + P_{rad}$, W_E = time-averaged electric stored energy, W_M = time-averaged magnetic stored energy, V = driving point voltage = tE averaged over the feed strip, t = dielectric thickness, $\omega = 2\pi f$.

If one were dealing with an *ideal* cavity, (one with no copper loss though perhaps with dielectric loss),

the impedance could also be computed by the expression

$$Z = [P+j2\omega(W_M - W_E)]/|I|^2 \tag{3}$$

or

$$Z = -V/I \tag{4}$$

where I = the total input current. However, in the case of microstrip antennas analyzed by the procedure just described, equations (2), (3), and (4) give different results. In fact, only equation (2) yields useful results, and then only for cases where excitation of the dominant mode is sufficiently strong. When this is not the case, equation (2) also fails. The reason for this failure and inconsistency can be traced to the fact that additional losses P_{rad}, P_{Cu}, and P_{sw} are only partially accounted for in equations (2) and (3) and not at all in equation (4) since E (and thus V) as given by equation (1) does not depend on all these losses. In order for all these expressions to agree, the poles of E in equation (1) must be modified to account for these additional losses.

It seems reasonable to modify the locations of the complex poles by some means so as to make all three expressions, (2), (3), and (4), coincide. This can be done by lumping all losses into a single "effective dielectric loss" with effective loss tangent δ_{eff}. Thus, in equation (1) and all the expressions for P, W_E, and W_M, the complex wave number k would be replaced by an effective wave number

$$k_{eff} = \sqrt{\epsilon_r(1-j\delta_{eff})}\,k_0.$$

The question now becomes how to compute δ_{eff}. A simple method is given below.

In an ideal cavity, the loss tangent is related to the quality factor, Q, by $\delta = 1/Q$. Therefore one can define $\delta_{eff} = 1/Q = P/(2\omega W_E)$. Since W_E and P depend on δ_{eff} in a very complex manner, strictly speaking, the solution of δ_{eff} to this non-linear equation is very involved. Fortunately, in the present computation, an accurate value of Q can still be obtained even though W_E and P are computed by simply using k for k_{eff}. This can be explained as follows. At resonance of say the $m=M$, $n=N$, mode, the E field, as clearly seen from equation (1),

is dominated by the MNth modal term. Thus W_E and P will assume the following form:

$$2\omega W_E = \frac{\alpha}{|k^2-k_{MN}^2|^2} + a, \quad P = \frac{\beta}{|k^2-k_{MN}^2|^2} + \mathrm{Re}\left\{\frac{\gamma}{k^2-k_{MN}^2}\right\} + b$$

The coefficients, α, β, and γ, and the contribution due to terms of all other (non-resonant) modes, a and b, can be derived from equation (1). They are somewhat lengthy but can be obtained in a straightforward manner and therefore are omitted for brevity. Thus near resonant frequencies,

$$\delta_{\mathrm{eff}} = 1/Q = \frac{P}{2\omega W_E} = \frac{\beta}{\alpha} + O(|k^2-k_{MN}^2|) \approx \frac{\beta}{\alpha}.$$

This result indicates that in a moderately high Q cavity, the exact value of k is not needed for evaluation of Q. Therefore it suffices to compute for frequencies in the region of each resonant mode the value of δ_{eff} (*i.e.* α, β with the aid of (1)) at the resonant frequency only. With δ_{eff} thus determined, the impedance locus can be efficiently computed by use of (4) and (1).

A parameter described as the "effective width" of the feed was employed in equation (1). For the case of a microstrip antenna fed by a strip line on its perimeter, the effective feed width is taken to be the physical width of the strip. However, if the microstrip is fed at a point interior to the patch by a coaxial cable, it is still convenient to think of the antenna as being fed by a uniform strip of vertically oriented electric current. However, due to the complicated fringing in the vicinity of the feed, the width of this "equivalent" feed will be different from the diameter of the center conductor of the coaxial feed. It is found that the impedance locus is unaffected by the orientation of the feed strip. Thus, in the case of the rectangle, the strip was always taken parallel to the x axis. In the disk, the strip was taken as a segment of the circle coaxial to the disk passing through the feed point. However, the degree to which the computed impedance locus is shifted into the upper half of the Smith chart is dependent somewhat on the actual width chosen for this effective feed. In general the narrower the feed, the more inductive the locus. At present, the effective width of the feed has been chosen by comparing the computed locus to measured locus for a point on the microstrip. Once this effective width is chosen, it is used at any other feed point in the antenna with good results as the next section will show. However, due to the difference in fringing when a coaxial feed is located directly on the edge of the microstrip than when in the interior, a separate effective

width should be determined for the former. In the case of the rectangular microstrip experiments carried out by the authors, an effective width of five times the diameter of the coaxial feed cable center conductor was used. Clearly this complex problem deserves a more rigorous and detailed analysis in its own right. This is currently under study by the authors.

III. *IMPEDANCE VARIATION*

This theory has been applied to study the variation of impedance with feed location for rectangular and disk microstrip antennas. Figures 1 and 3 show the respective results of the theory compared with the measurements. As can be seen, in all cases, both the shape of the locus and the distribution of frequencies on the locus (thus the Q) are in good agreement with the experiment. (It should also be noted that the frequencies have been corrected for the fringing field effect by edge extension using the formulas by Hammerstad [6] and Long and Shen [7] for the rectangular and circular microstrips, respectively.)

It is also clear from these two figures that the impedance locus can be varied over a wide range by simply changing the feed location. Since the pattern of the antenna is dependent mainly upon the field structure of the dominant mode only, the impedance can thus be varied for matching purposes independently of the pattern. The results also indicate that by using the appropriate effective feed width the theory can predict the locus very accurately for any feed location inside the antenna.

An observation of equation (1) shows that the antenna, so far as its impedance is concerned, can have a simple network representation. Define for convenience $\omega_{mn} = vk_{mn}/\sqrt{\epsilon_r}$. Then the impedance can be written as

$$Z = j\omega \frac{\mu_0 t v^2}{\epsilon_r} \sum_{m,n=0}^{\infty} \frac{\phi_{mn}^2(x',y') j_0^2(\frac{m\pi d}{2a})}{\omega_{mn}^2 - (1 - j\delta_{\text{eff}})\omega^2} = \sum_{m,n=0}^{\infty} \frac{1}{j\omega C_{mn} - j\frac{1}{\omega L_{mn}} + G_{mn}(\omega)} \tag{5}$$

where

$$G_{mn}(\omega) = \omega\delta_{\text{eff}}/\alpha_{mn}, \quad L_{mn} = \alpha_{mn}/\omega_{mn}^2, \quad C_{mn} = 1/\alpha_{mn},$$

and

$$\alpha_{mn} = \frac{\mu_0 t v^2}{\epsilon_r} \phi_{mn}^2(x',y') j_0^2(\frac{m\pi d}{2a})$$

The microstrip antenna is typically narrow band. Thus, over the band of the antenna operation at any mode

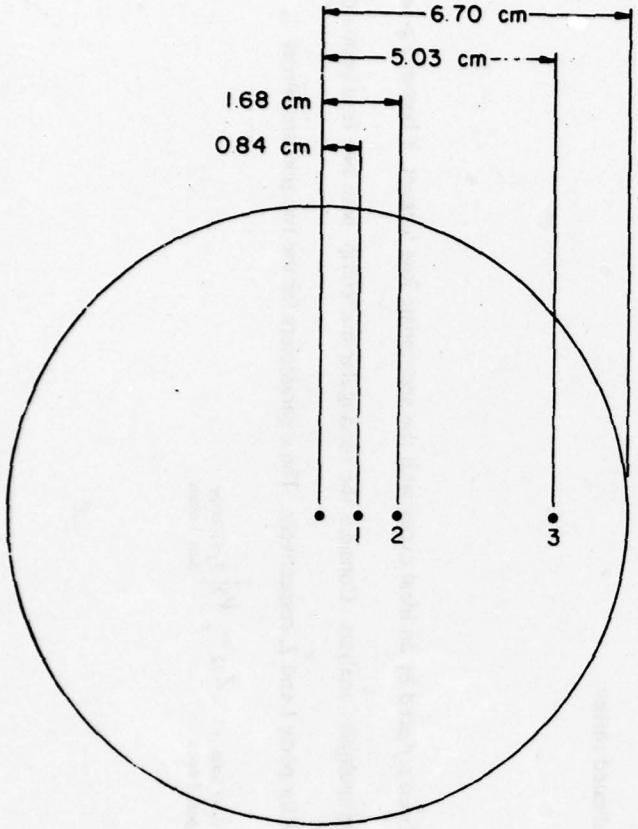

DISK MICROSTRIP ANTENNA

SUBSTRATE: REXOLITE 2200
1/16" NOMINAL THICKNESS

(a)

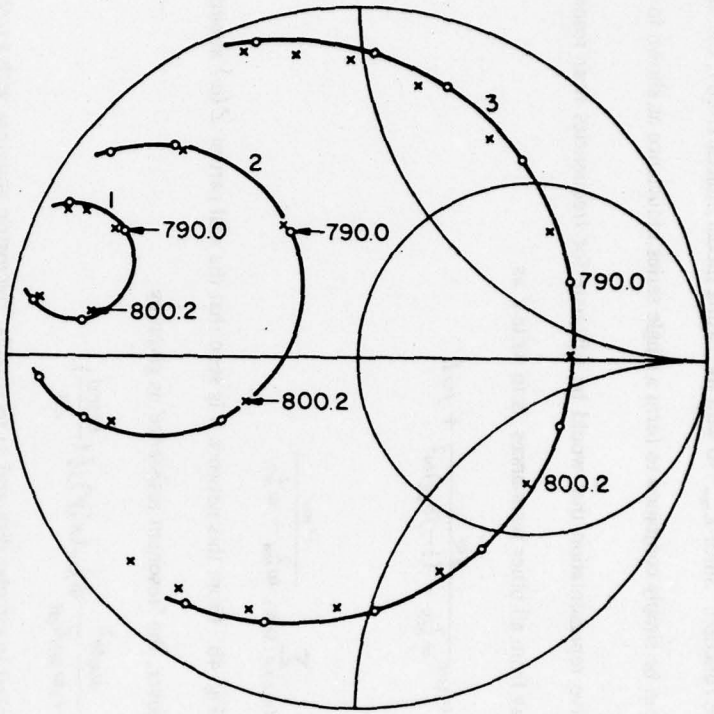

MEASURED LOCUS

COMPUTED LOCUS

INCREMENT: 5 MHz

(INCREASING FREQUENCY IS CLOCKWISE)

(b)

Fig. 3. (a) Dimensions and feed locations of circular disk microstrip antenna. (b) Measured and computed impedance loci.

(M,N), $G_{mn}(\omega)$ can be approximated simply by $G_{mn}(\omega_{MN})$. Thus, equation (5) represents a Foster expansion of a driving point impedance function. Since $L_{mn} \to 0$ with increasing modal indices (m,n), the infinite number of high-order Foster sections can be simply combined to form a single series inductance as shown in Fig. 4a.

A simpler alternative representation that would be adequate for frequencies near resonance of a mode (M,N), but sufficiently away from all other resonances, is to write Z as

$$Z \approx \alpha_{MN} \frac{j\omega}{\omega_{MN}^2 - (1-j\delta_{eff})\omega^2} + j\omega L'$$

where

$$L' = \sum_{(m,n)\neq(M,N)} \frac{\alpha_{mn}}{\omega_{mn}^2 - \omega_{MN}^2}.$$

This yields the network of Fig. 4b. From this network it is seen that the real part of $Z(\omega)$ attains its maximum at resonance, $\omega=\omega_{MN}$. Moreover, the "resonant resistance" is given by

$$\frac{1}{G_{MN}(\omega_{MN})} = \frac{\mu_0 t \nu^2}{\epsilon_r \omega_{MN} \delta_{eff}} \phi_{MN}^2(x',y') j_0^2\left(\frac{m\pi d}{2a}\right).$$

This equation has been applied to circular disk and to rectangular microstrip antennas with excellent results. Figures 5 a and b compare measured and computed resonant resistance *versus* feed location for the first and second resonant modes of a circular disk and rectangular microstrip antenna, respectively. It should be noted that these circuit representations differ from those reported by others [1,2,3] which are based on the over-simplified slot-transmission line approach as indicated earlier.

IV. *MULTIPORT ANALYSIS*

Once the antenna has been replaced by an ideal cavity with the appropriate loss tangent, it becomes a relatively simple matter to perform multiport analysis. Consider the rectangular microstrip with two feed points of coordinates (x_1,y_1) and (x_2,y_2) for ports 1 and 2, respectively. The z parameters for the two port are simply

$$Z_{11} = V_1\Big|_{\substack{I_1=1 \text{ amp,} \\ \text{port 2 open}}} \qquad Z_{22} = V_2\Big|_{\substack{I_2=1 \text{ amp,} \\ \text{port 1 open}}}$$

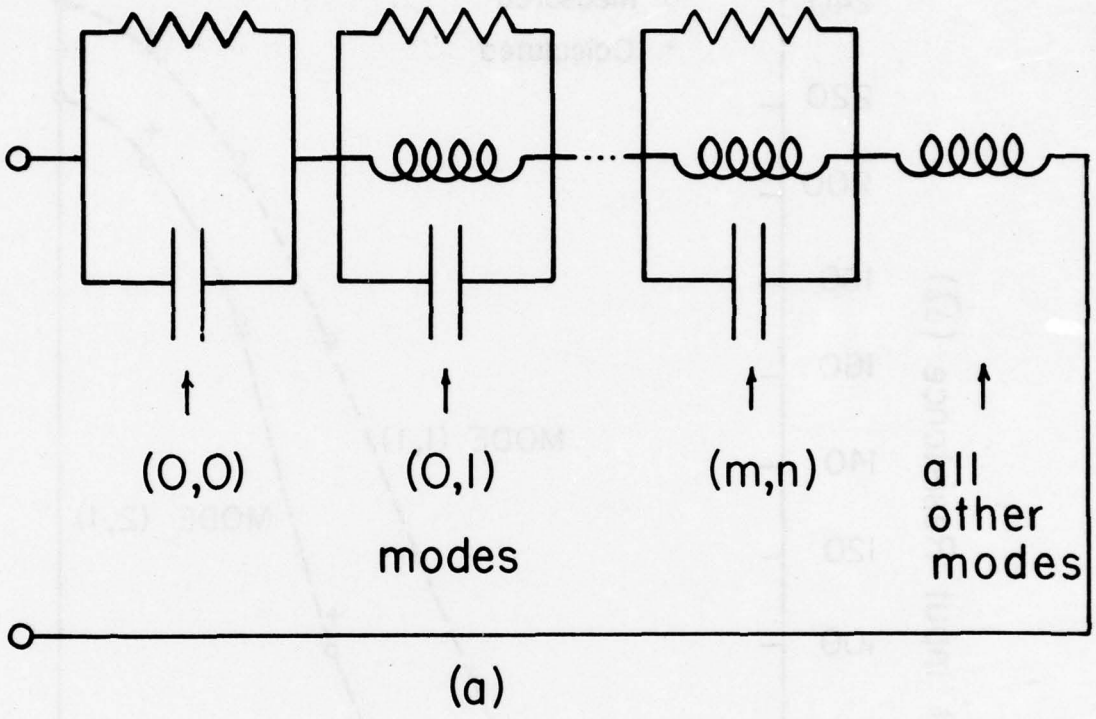

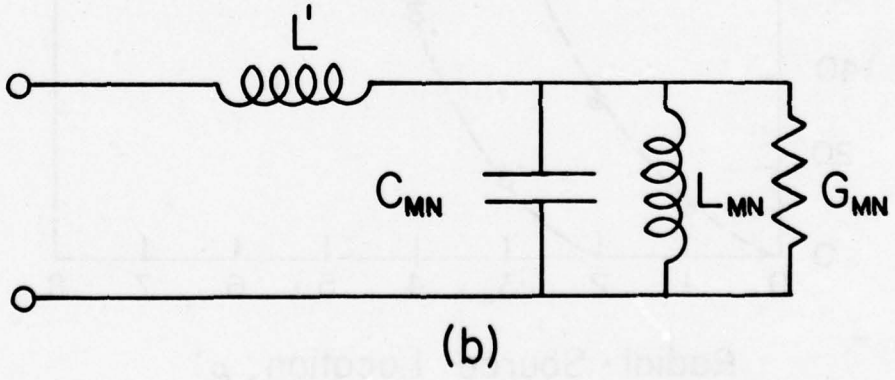

Fig. 4 (a) Network model for microstrip antenna operated in a band about the (M,N) mode.
(b) A simplified network model valid when ω_{MN} is well separated from all other resonant frequencies.

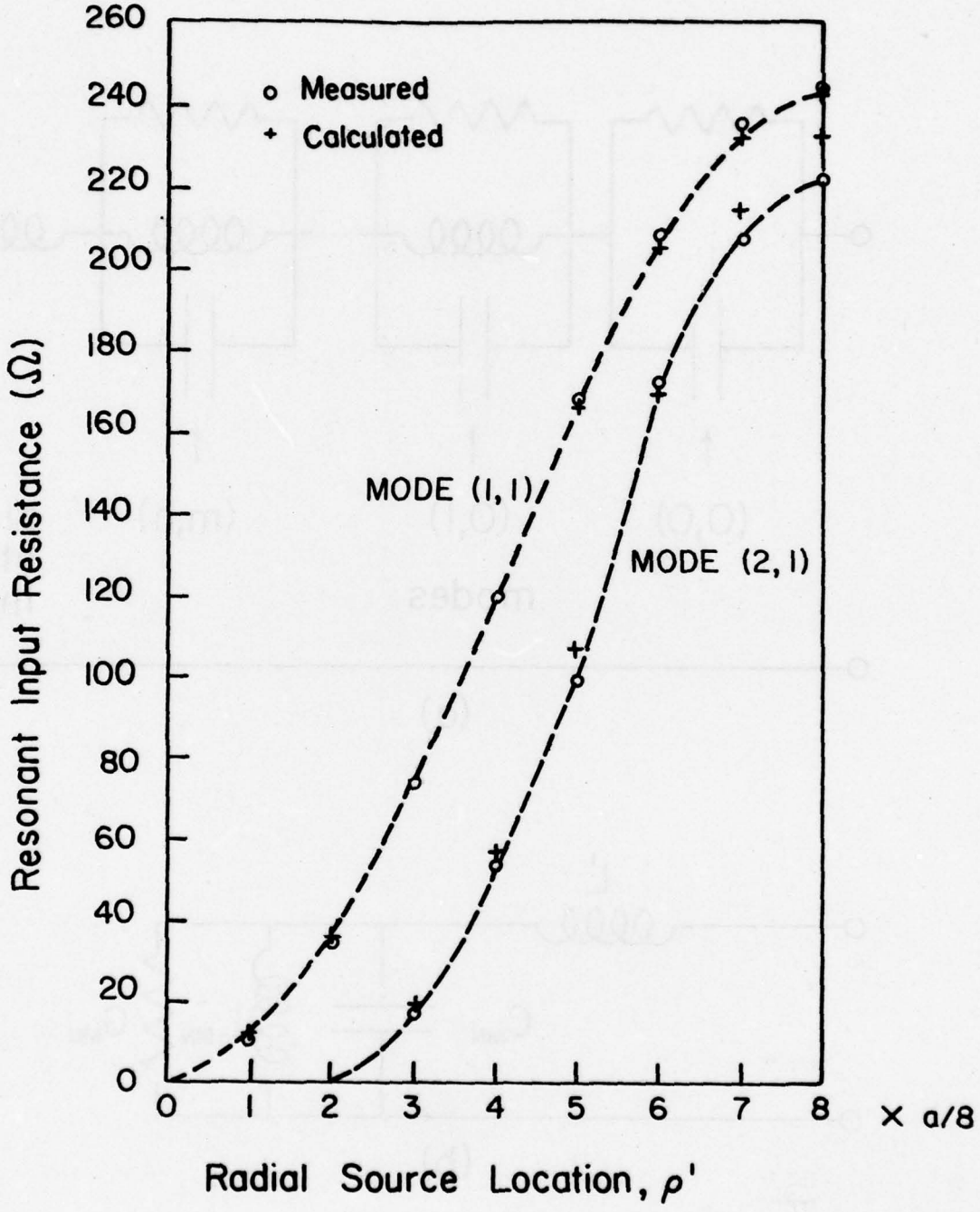

Fig. 5 (a) Variation of resonant resistance with feed location in circular disk microstrip antenna of radius a.

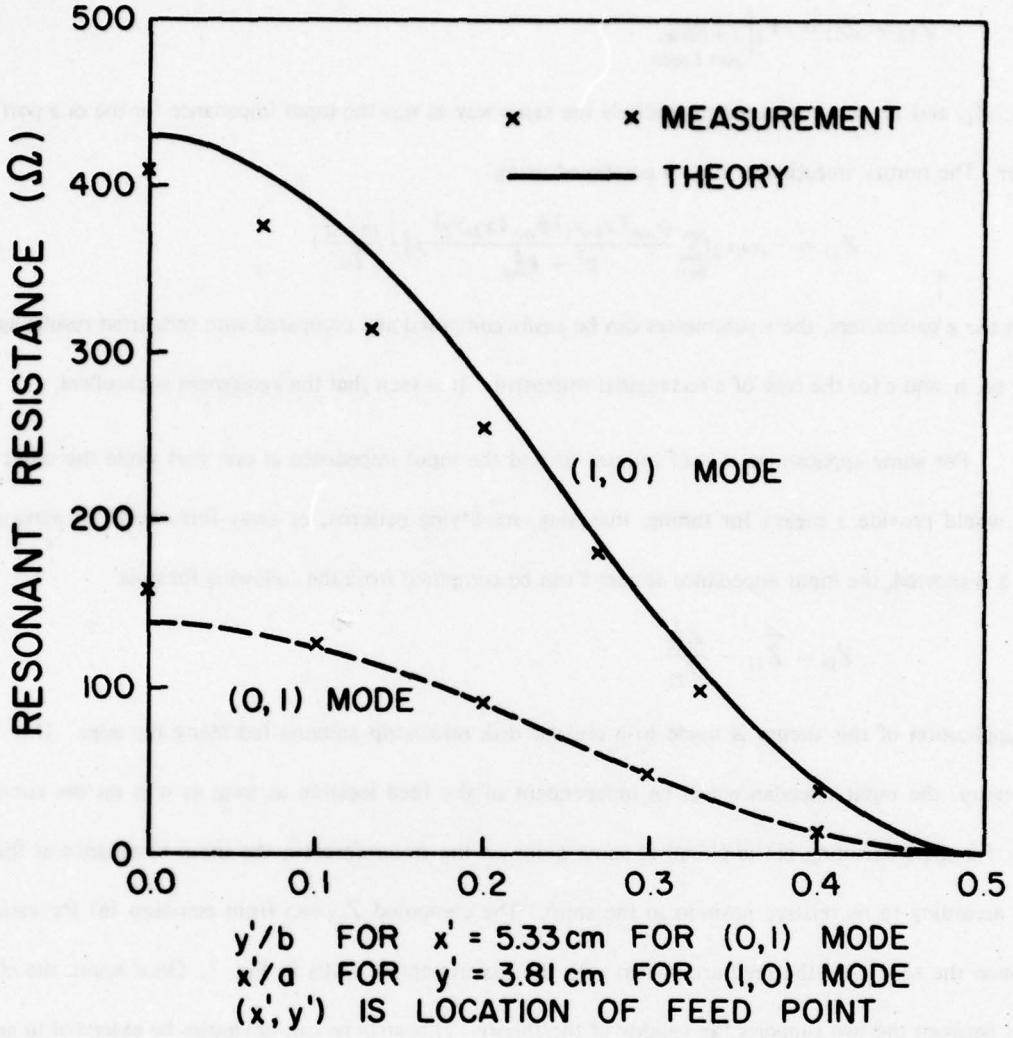

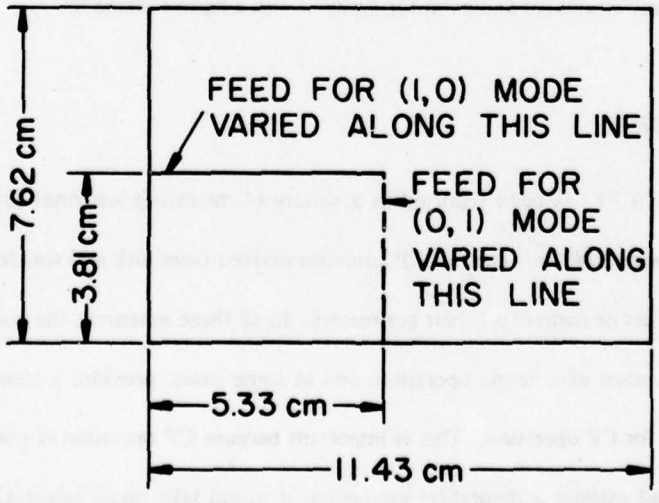

RECTANGULAR MICROSTRIP ANTENNA USING 1/16" REXOLITE 2200

Fig. 5 (b) Variation of resonant resistance with feed location in a rectangular microstrip antenna.

$$Z_{12} = Z_{21} = V_2 \Big|_{\substack{I_1 = 1 \text{ amp.} \\ \text{port 2 open}}} .$$

Thus, Z_{11} and Z_{22} are computed in precisely the same way as was the input impedance for the one port discussed earlier. The mutual impedance, Z_{12}, is computed using

$$Z_{12} = -j\omega\mu_0 t \sum_{m,n} \frac{\phi_{mn}(x_1,y_1)\phi_{mn}(x_2,y_2)}{k^2 - k_{mn}^2} j_0^2 \left(\frac{m\pi d}{2a}\right)$$

From the z parameters, the s parameters can be easily computed and compared with measured results as shown in Figs. 6a, b, and c for the case of a rectangular microstrip. It is seen that the agreement is excellent.

For some applications it is of interest to find the input impedance at one port while the other is loaded. This would provide a means for tuning, matching, modifying patterns, or array formation. In particular, when port 2 is shorted, the input impedance at port 1 can be computed from the following formula

$$Z_{in} = Z_{11} - \frac{Z_{12}^2}{Z_{22}} . \tag{6}$$

An application of this theory is made to a circular disk microstrip antenna fed along the edge. Due to circular symmetry, the input impedance will be independent of the feed location as long as it is on the circumference. Now if a short-circuiting pin is placed at some point on the circumference, the input impedance at the feed will vary according to its relative position to the short. The computed Z_{in} loci from equation (6) for various angles between the short and the feed are shown with the experimental results in Fig. 7. Once again, the close agreement between the two supports the validity of the theory. This analysis can obviously be extended to any number of ports for more complex array structures and even for systems with adaptive elements.

V. *CIRCULAR POLARIZATION*

Circular polarization (CP) has been reported in a variety of microstrip antennas [8], [9], [10]. Experimental work was recently reported [8] on a class of CP antennas derived from disk and square microstrip antennas by cutting slots in their interiors or corners off their perimeters. In all these antennas, the current theory provides an explanation for the mechanism of antenna operation, and in some cases, provides a means for predicting the necessary dimension needed for CP operation. This is important because CP operation is possible only for a very narrow band of frequency and without a theoretical prediction, it would take many painstaking cut-and-trials for

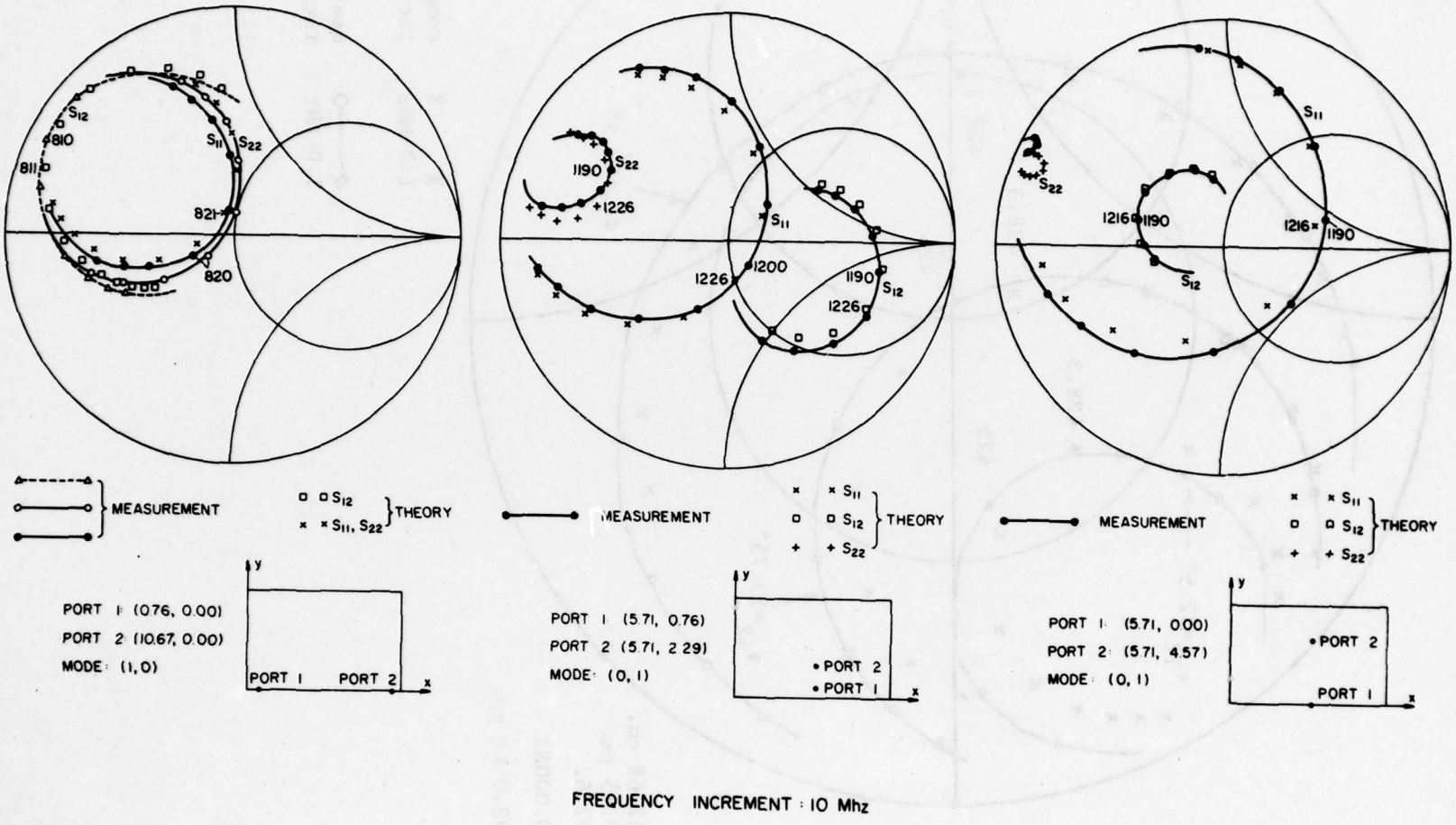

Fig. 6 Two port S parameters for a rectangular microstrip antenna with various feed locations as shown.

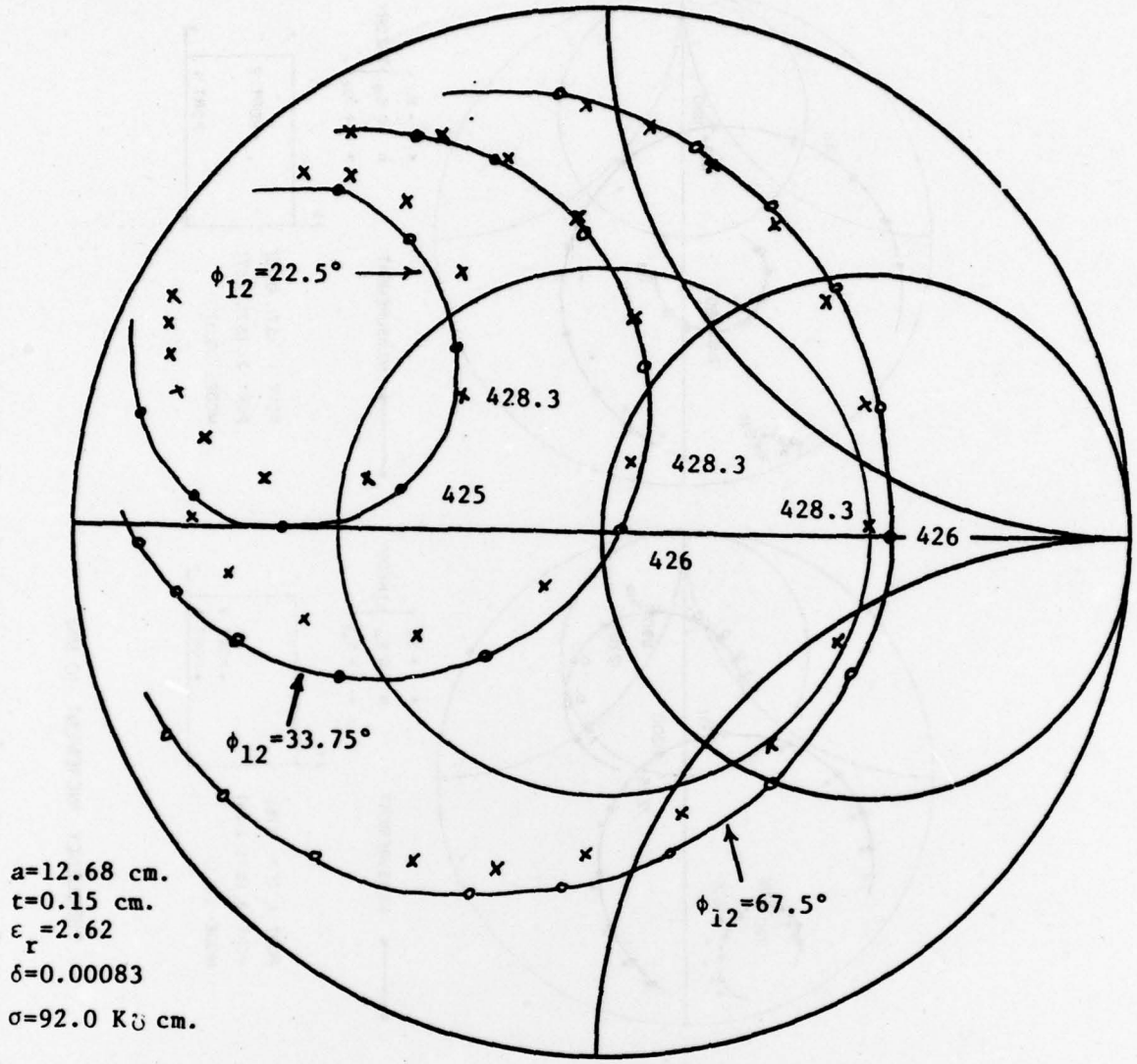

Fig. 7 The impedance variation for a disk microstrip antenna with feed and shorting stub on the circumference and at various values of angle ϕ_{12} between them.

reaching the correct dimensions.

Consider, as a first example, a *nearly square* microstrip of dimension $a \times b$ as shown in Fig. 8a. If $b+c=a$ where $c/b \ll 1$, then the resonant wave numbers of the mode (0,1), k_{01}, and of the mode (1,0), k_{10}, will be very close to one another. In fact, they will be close enough to assume that the effective loss tangent is the same for each of the two modes. Feeding the antenna at point 1 will excite the ϕ_{10} mode but not ϕ_{01}. Feeding at point 3 will excite ϕ_{01} but not ϕ_{10}. Feeding at point 2 or on the diagonal drawn in Fig. 8a will excite a dominant field proportional to $\psi_+=\phi_{01}+\phi_{10}$. With a feed at point 4, the excited field will be proportional to $\psi_-=\phi_{01}-\phi_{10}$. In the far field, in the direction perpendicular to the plane of the microstrip, the electric fields produced by ϕ_{01} and ϕ_{10} are polarized in the x and y directions, respectively, and can be written for appropriate choice of input current magnitude and phase as

$$E_x \approx \frac{\cos(\pi x'/a)}{k^2 - k_{10}^2}, \quad E_y \approx \frac{\cos(\pi y'/b)}{k^2 - k_{01}^2} \tag{7}$$

The contributions of the non-resonant modes are ignored in (7) for frequencies near the resonances of the two modes. To obtain CP in the direction of the zenith, the ratio of E_y to E_x should be $e^{\pm j\pi/2}$. Define $A=\cos(\pi y'/b)/\cos(\pi x'/a)$. Then

$$\frac{E_y}{E_x} \approx A\frac{k^2 - k_{10}^2}{k^2 - k_{01}^2} \approx A\frac{k - k_{10}}{k - k_{01}}. \tag{8}$$

It is particularly illuminating to plot k, k_{01}, and k_{10} in the complex k plane as was done in Fig. 9. For E_y/E_x to be $e^{j\pi/2}$, equation (8) requires that

$$\Delta k = k_{01} - k_{10} = L(A + \frac{1}{A}). \tag{9}$$

But

$$\frac{L}{\bar{k}} \approx \frac{1}{2}\delta_{\text{eff}} = \frac{1}{2Q}, \tag{10a}$$

$$k_{01} - k_{10} = \frac{\pi}{b} - \frac{\pi}{a} = \frac{\pi}{b} - \frac{\pi}{b+c} \approx \frac{\pi c}{b^2}, \tag{10b}$$

$$\bar{k}b \approx \pi. \tag{10c}$$

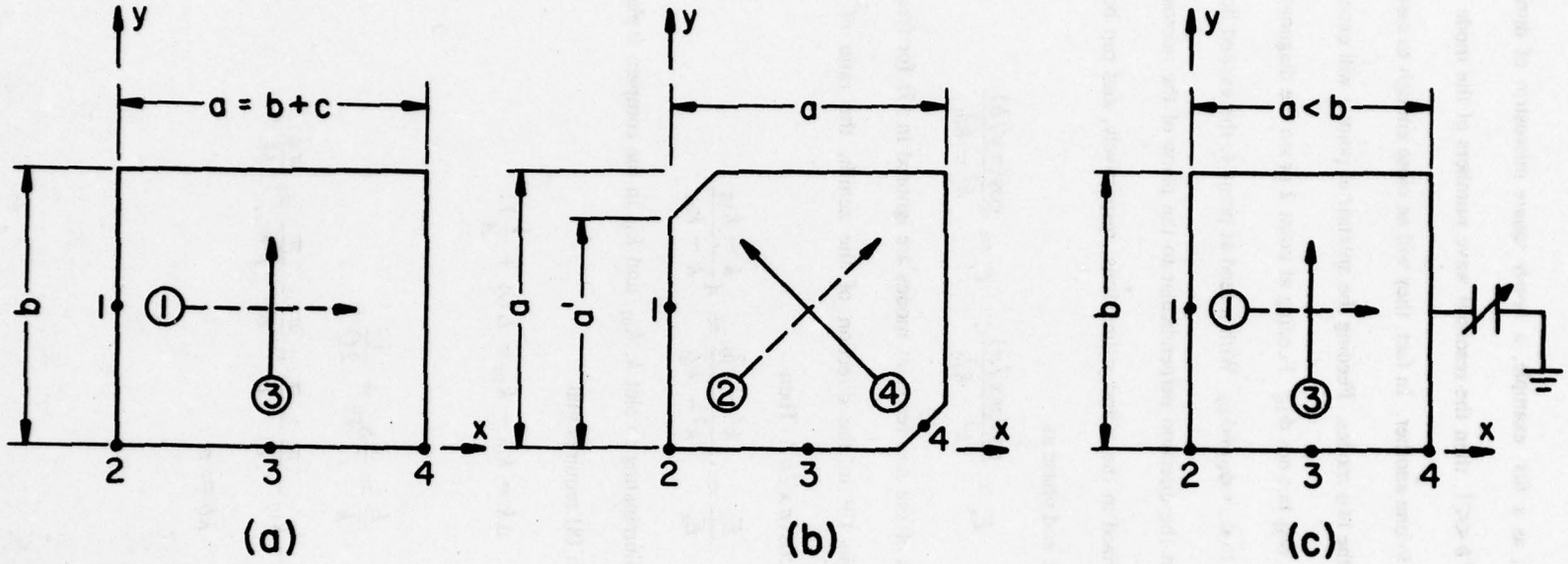

Fig. 8 Microstrip antennas capable of producing circular polarization
(a) Nearly square microstrip.
(b) Truncated microstrip.
(c) Capacitively loaded microstrip.

Polarization of the far field in the Z-direction (zenith) is indicated by either a solid or a dashed arrow with a circled number corresponding to the feed location number.

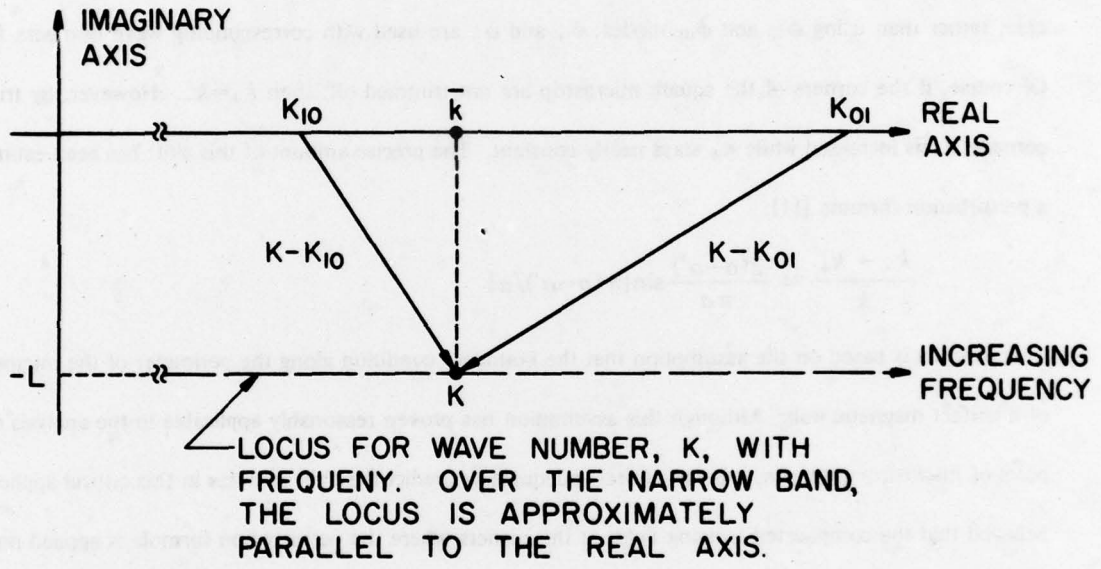

Fig. 9 Relative pole positions in the complex K plane.

(The parameters $\bar{k}$ and L are defined in Fig. 9.) Thus, combining (9) with (10),

$$\frac{\Delta k}{\bar{k}} = \frac{k_{01} - k_{10}}{\bar{k}} \approx \frac{c}{b} \approx \frac{A + \frac{1}{A}}{2Q} .$$

For the case of the feed point taken on the diagonal of the microstrip, $A=1$ and therefore

$$\frac{a}{b} = 1 + \frac{1}{Q} .$$

The sense of rotation of the CP wave produced by the antenna fed at point 2 will be left hand circularly polarized. By simply feeding at point 4 instead, the sense is reversed.

For the antenna of Fig. 8b, the analysis follows along the same lines as that for Fig. 8a. However, in this case, rather than using ϕ_{10} and ϕ_{01} modes, ψ_+ and ψ_- are used with corresponding wave numbers k_+ and k_-. Of course, if the corners of the square microstrip are not trimmed off, then $k_+=k_-$. However, by trimming the corners, k_- is increased while k_+ stays nearly constant. The precise amount of this shift has been estimated using a perturbation formula [11]:

$$\frac{k_- - k_+}{\bar{k}} \approx \frac{2(a-a')}{\pi a} \sin[\pi(a-a')/a]$$

This formula is based on the assumption that the boundary condition along the perimeter of the microstrip is that of a perfect magnetic wall. Although this assumption has proven reasonably applicable to the analysis of most aspects of microstrip antennas, it is not entirely adequate to predict the shift in poles in this critical application. It is believed that the complicated fringing fields at the corners where the perturbation formula is applied make the approximation of insufficient accuracy in this application. However, one can *experimentally* refine the proper dimensions by simply measuring the resonant frequencies corresponding to k_+ and k_- by feeding at ports 2 and 4, respectively.

The antenna in Fig. 8c operates by the same mechanism as that in 8a. In this case, however, the pole k_{10} can be varied by simply adjusting the capacitance attached to the antenna. (Since the capacitor is located at $y=b/2$, a null of the ϕ_{01} mode, k_{01}, is unaffected by the capacitor.) If the range of capacity is large enough, and $a<b$, one is able to adjust the antenna to produce fields of practically any polarization and sense. Thus the antenna can be at one moment left hand CP, linear at the next, and right hand CP at some other time by simply changing the capacitance (or the bias on a varactor diode). It should be noted that the capacitor could just as well

have been located in the corner of the antenna in which case one would feed at points 1 or 3 to achieve CP operation.

Figures 10a, b, and c show the respective measured patterns obtained from the three antennas of Fig. 8. The patterns are taken in a plane perpendicular to the microstrip and are measured with a rotating dipole. It is clear that all three patterns yield excellent CP for a cone of large solid angle centered about the z axis.

Other structures that utilize a single feed point have been reported to produce CP. They are disk antennas with slots [8] and a pentagonal shaped antenna [10]. These too are believed to operate by the same mechanism as described for the rectangular antenna. Although all these antennas are able to produce good CP without the need of an external phase-shifter and power divider, a distinct advantage, it is clear from the theory given above that their CP operation is *extremely narrow band.* Figure 11 shows the degradation in axial ratio with normalized frequency defined as

$$\xi = \frac{\omega - \bar{\omega}}{\omega_{01} - \omega_{10}} \text{ where } \bar{\omega} = v\bar{k}$$

Thus, for an axial ratio within 3 dB (at zenith) which would produce a polarization mismatch loss of less than 1/4 dB with respect to CP, one is limited to a bandwidth of about 35% of the frequency difference between the two dominant poles or about $35/Q$ percent bandwidth. Typically, Q is on the order of 50-100 so that the bandwidths of less than 1 percent are to be expected thus limiting the usefulness of this method of producing CP.

VI. *CONCLUSION*

A simple and efficient theory is established to analyze the behavior of microstrip antennas with remarkable accuracy even if the dominant mode is not strongly excited. Several important applications which require a theory of high accuracy are presented. The input antenna impedance can be varied over a wide range for matching purposes simply be changing the feed location. The confidence in the theory is particularly strengthened when it predicted correctly the extremely critical antenna dimensions for producing circular polarizations. The theory is also applied to multiport antenna configurations. For nearly all the cases considered, theoretical and experimental

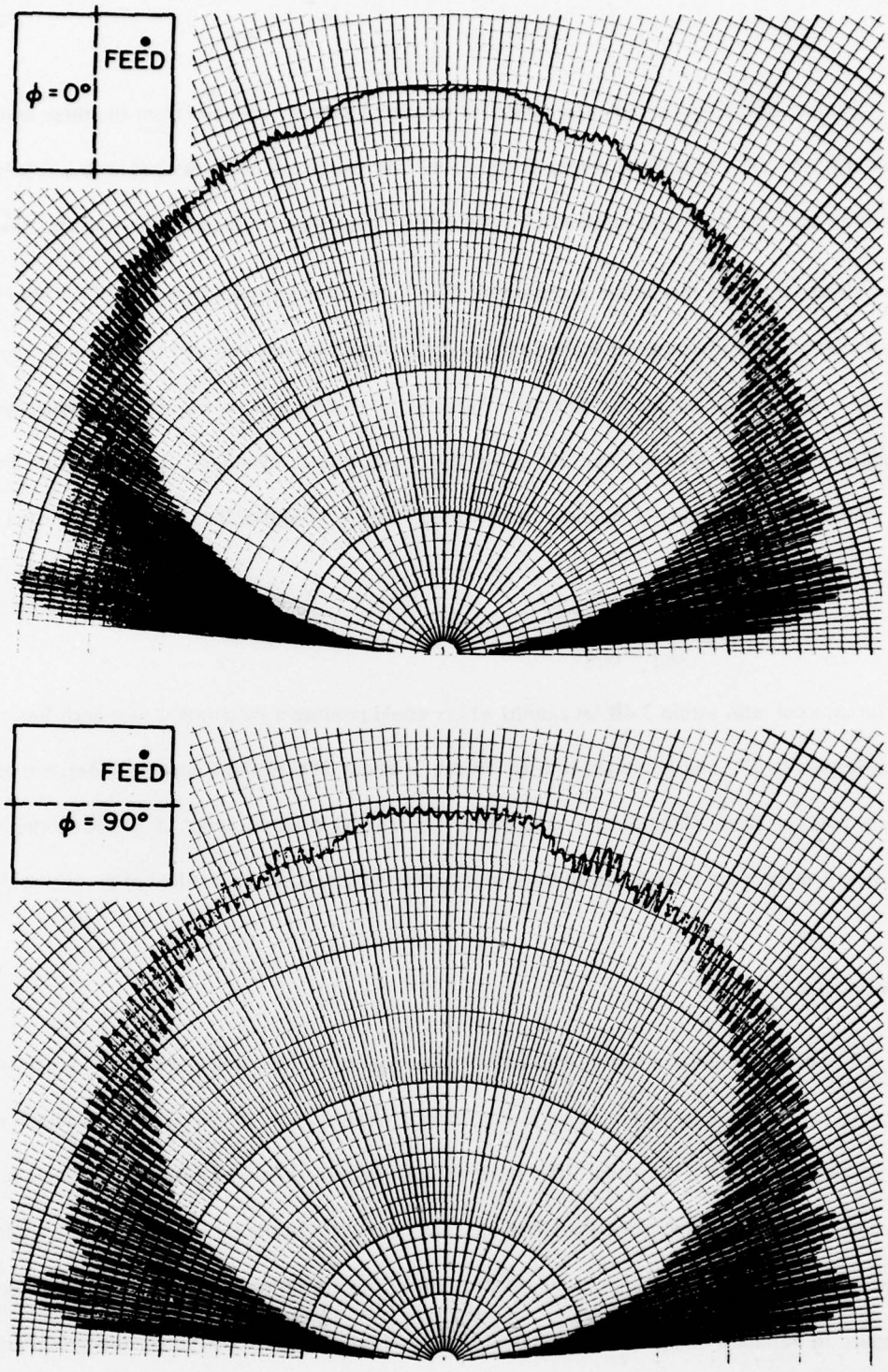

Fig. 10 Elevation patterns taken with rotating dipoles for (a) nearly square microstrip antenna

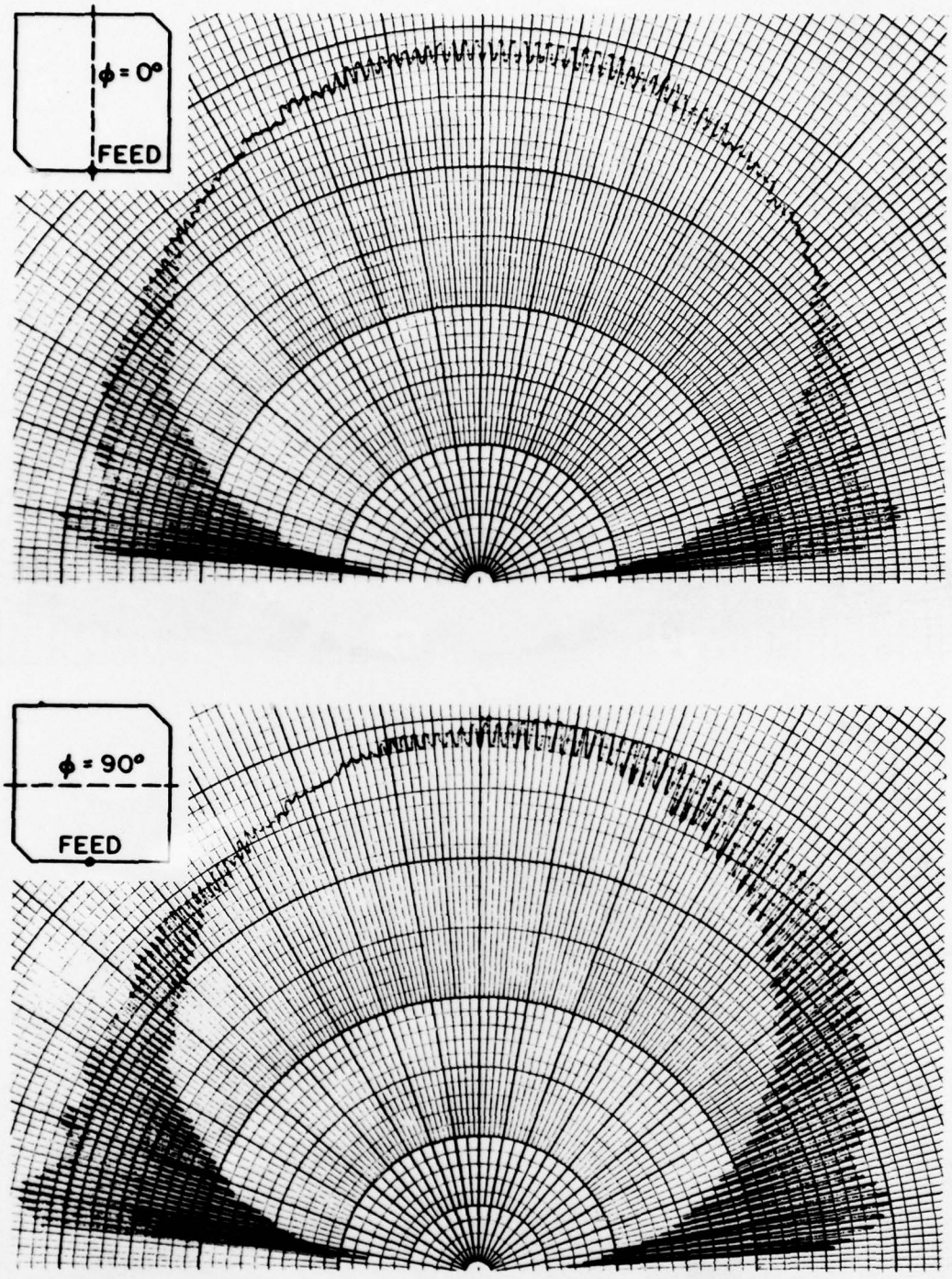

Fig. 10 (b) truncated microstrip antenna, and

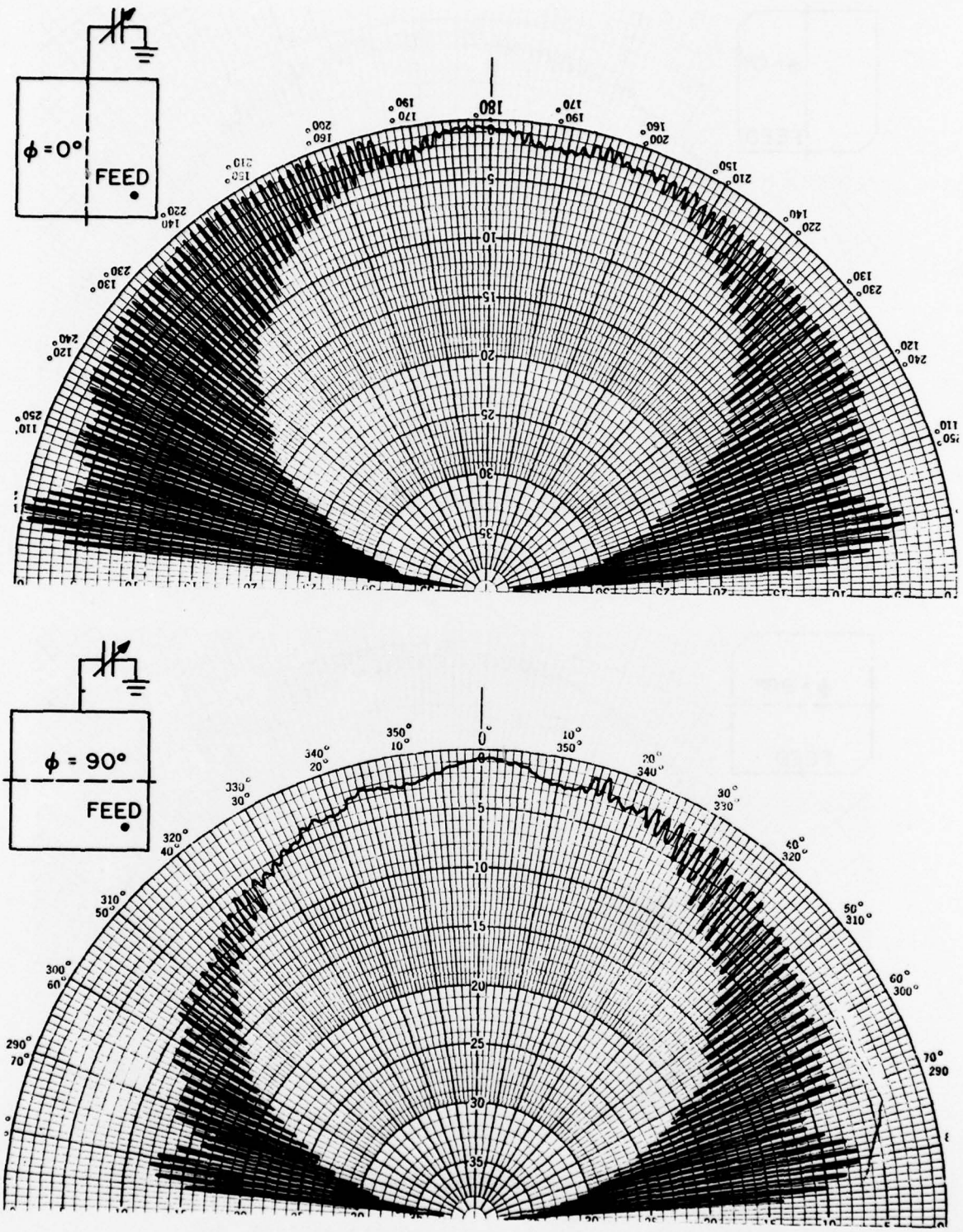

Fig. 10 (c) capacitively loaded microstrip antenna.

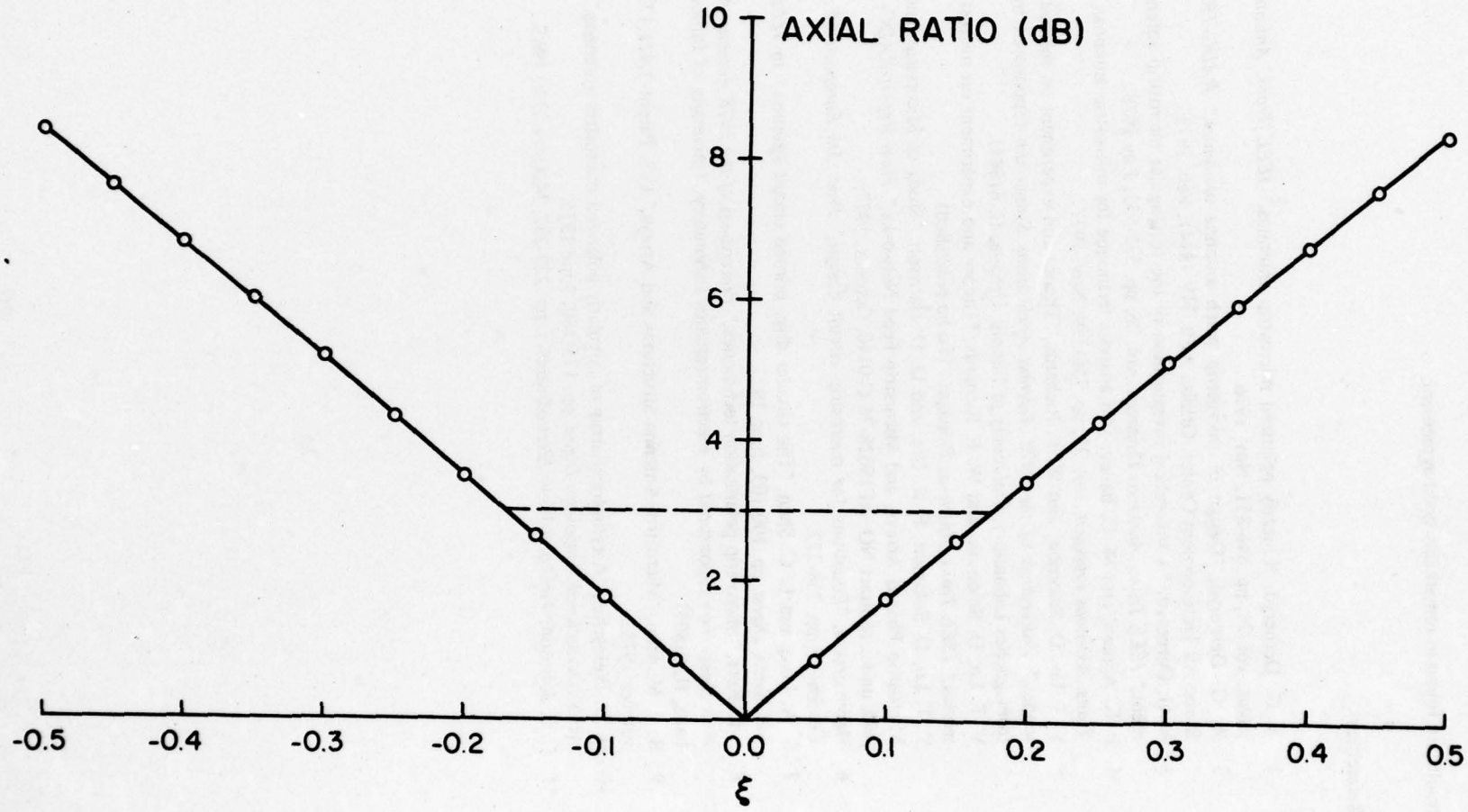

Fig. 11 Degradation of axial ratio with normalized frequency.

results are found in remarkably good agreement.

References

1 A. G. Derneryd, "Linearly polarized microstrip antennas," *IEEE Trans. Antennas Propagat.*, vol. 24, pp. 846-851, Nov. 1976.

2 A. G. Derneryd, "Design of microstrip patch antenna elements," *RADC-TR-78-46*, Rome Air Development Center, Griffiss AFB, NY 13441, Feb. 1978.

3 A. G. Derneryd, "A theoretical investigation of the rectangular microstrip antenna element," *IEEE Trans. Antennas Propagat.*, vol. 26, pp. 532-533, July 1978.

4 P. K. Agrawal and M. C. Bailey, "An analysis technique for microstrip antennas," *IEEE Trans. Antennas Propagat.*, vol. 25, pp. 756-759, Nov. 1977.

5 Y. T. Lo, D. Solomon, and W. F. Richards, "Theory and experiment on microstrip antennas," *Proceedings of the 1978 Antenna Applications Symposium* (Sponsored by Electromagnetics Laboratory, University of Illinois, Urbana, IL 61801)
Y. T. Lo, D. Solomon, and W. F. Richards, "Theory and experiment on microstrip antennas," *IEEE Trans. Antennas Propagat.*, (To be published)
Y. T. Lo, D. Solomon, F. R. Ore, and D. D. Harrison, "Study of Micorstrip Antennas, Microstrip Phased Arrays, and Micorstrip Feed Networks," *Final Report RADC-TR-77-406*, under contract NO. AF19628-76-C-0140, October, 1977.

6 Hammerstad, "Equations for microstrip circuit design," *Proc. 5th European Microwave Conference*, pp. 268-272.

7 S. A. Long and L. C. Shen, "The circular disc, printed circuit antenna," in *IEEE AP-S Intl. Symp. Digest*, pp. 100-103, June 1977.

8 J. L. Kerr, "Microstrip polarization techniques," *Proceedings of the 1978 Antenna Applications Symposium* (Sponsored by Electromagnetics Laboratory, University of Illinois, Urbana, IL 61801)

9 R. E. Munson, "Microstrip Antenna Structures and Arrays," U.S. Patent 3,921,177, November 1975.

10 H. D. Weinschel, "A cylindrical array of circularly polarized microstrip antennas," *IEEE AP-S International Symposium Digest*, pp. 175-180, June 1975.

11 C. C. Johnson, *Field and Wave Electrodynamics*, pp. 229-232, McGraw Hill, 1965.

MISSION
of
Rome Air Development Center

RADC plans and executes research, development, test and selected acquisition programs in support of Command, Control Communications and Intelligence (C^3I) activities. Technical and engineering support within areas of technical competence is provided to ESD Program Offices (POs) and other ESD elements. The principal technical mission areas are communications, electromagnetic guidance and control, surveillance of ground and aerospace objects, intelligence data collection and handling, information system technology, ionospheric propagation, solid state sciences, microwave physics and electronic reliability, maintainability and compatibility.

Printed by
United States Air Force
Hanscom AFB, Mass. 01731